Adaptive introgression during environmental change can weaken reproductive isolation

Gregory L. Owens[1]*, *Kieran Samuk*[2]

[1] Department of Integrative Biology, University of California, Berkeley.
Berkeley, California, USA, 94720.

[2] Department of Biology, Duke University.
Durham, NC, USA, 27708.

*Corresponding author, gregory.lawrence.owens@gmail.com

Abstract

Anthropogenic climate change is an urgent threat to species diversity. One aspect of this threat is the collapse of species reproductive barriers through increased hybridization. The primary mechanism for this collapse is thought to be the weakening of ecologically-mediated reproductive barriers, as demonstrated in many cases of "reverse speciation". Here, we expand on this idea and show that adaptive introgression between species adapting to a shared, moving climatic optimum can readily weaken *any* reproductive barrier, including those that are completely independent of climate. Using genetically explicit forward-time simulations, we show that genetic linkage between alleles conferring adaptation to a changing climate and alleles conferring reproductive isolation (intrinsic and/or non-climatic extrinsic) can lead to adaptive introgression facilitating the homogenization of reproductive isolation alleles. This effect causes the decay of species boundaries across a broad and biologically-realistic parameter space. We explore how the magnitude of this effect depends upon the rate of climate change, the genetic architecture of adaptation, the initial degree of reproductive isolation, the degree to which reproductive isolation is intrinsic vs. extrinsic, and the mutation rate. These results highlight a previously unexplored effect of rapid climate change on species diversity.

Introduction

Global climate change (GCC) is expected to be an increasingly important stressor in the next century (Thomas et al. 2004, Hoffmann and Sgro 2011). GCC can lead to

significant fitness costs or extinction if populations cannot adjust their ranges (e.g. via migration) or adapt to the changing climate (Jump and Penuelas 2005; Zimova et al. 2016). Apart from its direct effects on species fitness, GCC can also profoundly alter the basic ecological functioning of ecosystems e.g. via changes in phenology or species composition (Walther et al. 2002). As such, GCC represents an existential threat to biological diversity, at the level of populations, species, and ecosystems. Considering the central role of biological diversity in the functioning of evolutionary and ecological processes, understanding the full biological effect of GCC remains a key problem.

One potential effect GCC is increased interspecies hybridization, which can itself precipitate further loss of biodiversity (Rhymer and Simberloff 1996, Todesco et al. 2016). Such hybridization can cause a common species to subsume a rare species (Oliveira et al. 2008; Beatty et al. 2014; Vallender et al. 2007) or the collapse of multiple species into a single hybrid swarm (Taylor et al. 2006). In both cases, genetic and species diversity are lost. GCC may also precipitate the collapse of species boundaries by breaking down spatial, temporal or behavioural premating barriers (Chunco 2014). At the simplest level, range shifts can bring together species that may have no other significant barriers (e.g. Garroway et al. 2010). Reproductive barriers relying on the timing of life-history events are also susceptible to climate change which can increase the temporal overlap between species (e.g. Gerard et al. 2006). Furthermore, behavioural isolation may rely on environmental cues disrupted by GCC, as in spadefoot toads in which water conditions influence mate choice (Pfennig 2007). The breakdown of these barriers may lead to loss of more rare species under GCC, or the collapse of sister

55 species, as has been seen in smaller localized environmental shifts (Taylor et al. 2006;
56 Vonlanthen et al. 2012).

57 While perhaps unfamiliar to many workers in the field of climate change science,
58 there is a rich theoretical literature dedicated to the study of the dynamics of
59 interspecific hybridization and gene flow (reviewed in e.g. Abbot 2013 and Seehausen
60 2013). Often framed in the context of the evolution and maintenance of reproductive
61 isolation (i.e. speciation), this literature has provided many key insights germane to the
62 study of climate change induced hybridization. For example, hybrid zone models have
63 shown that universally adaptive alleles readily introgress across hybrid zones, while
64 alleles that cause reproductive isolation generally resist introgression (Barton 1979,
65 Gompert et al. 2012, Barton 2013). Other modelling efforts have revealed that depending
66 on the balance between reproductive isolation and shared ecological selection,
67 introgression can cause previously isolated populations to remain isolated or collapse
68 into hybrid swarms (e.g. Buerkle 2000). Further, the balance between divergent natural
69 selection, gene flow and reproductive isolation has been extensive explored in the
70 theoretical speciation literature (see Barton 2013 and references therein). However there
71 has thus far been poor integration between models of reproductive isolation and models
72 of adaptation to climate change.

73 The fact that introgression can transfer alleles between species has led to the
74 idea that hybridization could facilitate adaptation to GCC through the transfer of
75 adaptive alleles between species, i.e. adaptive introgression. This has traditionally been
76 studied in the context of species/populations with pre-existing differential adaptation to
77 the changing climate variable; for example a warm adapted species transfering alleles to

a cold adapted species (e.g. Gómez et al. 2015). In this example, one species acts as a pool of alleles preadapted to a future climatic optimum. Importantly, in these types of models, introgression is being driven by selection and not demographic processes or perturbations of prezygotic isolation, as seen in other models where climate change drives hybridization.

What has not been appreciated in previous models of adaptation to a changing climate is that during a rapid environmental shift, segregating variation within two reproductively isolated species could theoretically undergo adaptive introgression even if neither species is particularly preadapted to the environmental shift. We propose that climate-induced adaptive introgression could readily occur in most species because (1) the identity of the particular alleles involved in climatic adaptation are likely idiosyncratic in each species/population, and (2) these alleles could, in principle, be globally adaptive under a GCC scenario. Indeed, segregating climate adaptation alleles (or linked blocks of alleles) could easily be strong enough to outweigh the fitness costs of any linked reproductive isolation alleles. As a side effect, reproductive isolation alleles could readily be homogenized between species, reducing reproductive isolation and precipitating the collapse of species boundaries. This scenario dramatically increases the likelihood of GCC-induced introgression from populations differing in altitude or latitude, to nearly any parapatric pair capable of hybridization, even if reproductive isolation is initially high.

Here, we direct testly of the role of climate-induced adaptive introgression in degrading reproductive barriers using state-of-the-art forward time population genetic computer simulations. We envision a scenario in which two species are initially

reproductively isolated (but capable of limited hybridization) and must cope with an extreme shift in the environment. We explore the parameter space under which adaptation to a shifting climatic optimum drives a reduction in reproductive isolation. We interpret these results in the context of the future anthropogenic climate change and the loss of species diversity.

Methods

Conceptual model

We consider the scenario of two parapatric species inhabiting demes in two different habitats. These species exchange migrants at a low level, but reproductive isolation via local adaptation (i.e. extrinsic postzygotic isolation and immigrant inviability) is strong enough to prevent substantial introgression. We imagine that these two species must also cope with constant adaptation to a shared oscillating "climate" optimum. This climatic optimum does not not directly affect the degree of local adaptation and/or reproductive isolation, i.e. reproductive isolation is completely independent of the direct effects of climate. The climate oscillation continues for a long initial burn in period, during which alleles conferring adaptation to climate accumulate in each species. After this period, the oscillation ends and the climatic optimum begins rapidly increasing at a constant rate, as is expected under projections of anthropogenic climate change.

We hypothesize that if the rate of change in the climatic optimum is sufficiently high, selection for migrant alleles conferring increased climate tolerance will overwhelm the negative fitness effects of linked reproductive isolation alleles. This will

123 cause the erosion of reproductive isolation between species and increase the chance of
124 speciation reversal. Importantly, we expect this outcome even when the strength of
125 ecological selection mediating reproductive isolation itself is orthogonal to the strength
126 of climate-mediated selection.
127
128 *Model details*
129 We implemented the above conceptual model as a genetically explicit Wright-
130 Fisher model in SLiM 3.0 (Haller and Messer 2018). As in all Wright-Fisher models,
131 population sizes are constant, all fitness is relative and extinction is impossible. The
132 details of our implementation are depicted graphically in Figure 1 and a list of
133 simulation parameters and their values are detailed in Table 1. We simulated two
134 diploid populations of constant size *Ne,* with a constant migration rate of *m* proportion
135 migrants per generation. Each individual was initialized with 99999 genetic loci
136 contained on a single chromosome with a uniform recombination rate of *r* between loci.
137 We initially scaled the recombination rate so that the entire genome was 100 cM in
138 length, but also explored varying recombination rates up a genome size of 1000 cM (see
139 Results). We modelled local adaptation in the two populations as l_{EX} divergently
140 selected alleles at loci evenly spaced across the chromosome, with each population fixed
141 for a different allele. Divergently selected alleles imposed a fitness cost of s_{RI} when not
142 found in their home population/habitat, modelling extrinsic postzygotic isolation.
143 In addition to extrinsic postzygostic isolation, we also modelled intrinsic
144 postzygotic isolation using two-locus Bateson-Dobzhansky-Muller incompatibilities
145 (Bateson 1909, Dobzhansky 1936, Muller 1942). These epistatic incompatibilities were

146 modelled as a fitness cost of s_{RI} scaled by the number of negatively-interacting pairs of
147 alleles from each population (see Supplementary Appendix 1 for details). When testing
148 the effects of BDMs, we maintained a constant number of total reproductive isolation
149 loci, but varied the proportion of loci that were extrinsic or BDM loci (l). We also
150 explored the effect of the total number of RI loci (i.e. the genetic architecture of RI *per*
151 *se*) on the potential for adaptive introgression/hybridization. To keep the total
152 magnitude of RI similar between simulations, we always co-varied s_{RI} so that the s_{RI} x l
153 was held constant. To allow for fine-scale view of introgression, we tracked ancestry
154 was using 100 neutral alleles initially fixed between the populations, spread evenly
155 across the genome. All alleles of selective/phenotypic effect were codominant with
156 dominance = 0.5.

157 In addition to reproductive isolation, individual fitness also depended on their
158 phenotypic distance from a climatic optimum. This optimum was initially 0, and during
159 the burn in period oscillated from -5 to 5 (in arbitrary units) every 500 generations based
160 on the formula: $sin(\pi * generation / 500) /5$. The individual phenotype was determined by
161 alleles at QTL-like climate loci which could appear via mutation at all sites other than
162 RI or ancestry tracking loci (i.e. 99899 - l sites). Climate QTL mutations occurred at a
163 rate μ per locus per sample per generation and their phenotypic effect was drawn from a
164 gaussian distribution with a mean of zero and a standard deviation of QTL_{SD}.
165 Conceptually, these QTL climate alleles modify whether an individual is “hot” (positive
166 effects) or “cold” (negative effects) adapted.

167 The first step of the simulations was a burn-in of 10Ne generations to simulate
168 the generation of standing genetic variation under normal climatic conditions. At the

end of the burn-in period, the complete state of each replicate simulation was saved. Each simulation was then continued under both a "control" and climate change scenario for an additional 100 generations. In the control scenario, the environmental oscillation continued as normal. In contrast, under the climate change scenario the phenotypic optimum increased by a rate of Δ each generation without oscillation. In each generation we recorded the average degree of reproductive isolation, mean fitness, the mean and standard deviation of the climate phenotype and the amount of introgressed ancestry for each population. Reproductive isolation (RI) was calculated accounting for the extrinsic and BDM loci. For extrinsic loci, RI was the difference in fitness for an average individual in their home habitat vs. the foreign habitat. For BDMs, since fitness penalties occur only in F1 hybrids and beyond, we calculated the expected average magnitude of BDM fitness costs based on Hardy-Weinberg expectations in F1s (Supplementary Appendix 1). Finally, for each simulation we report the mean introgressed ancestry and reproductive isolation between the start and end of control and test scenarios, as well as the mean rate of phenotypic change in Haldanes for the test scenario. A Haldane is a measure of evolutionary change in log mean trait value in units of standard deviation of that log trait (Gingerich 1993). All formulas used in the simulation are presented in the Supplementary Appendix and all code for underlying simulations is available at https://github.com/owensgl/adaptive_introgression.

To explore the parameter space under which adaptive introgression mediates RI collapse, we systematically varied the following parameters: mutation rate (μ), migration rate (m), strength of divergent selection (s_{RI}), the number of divergently selected loci (n_{RI}),

192 the proportion of BDMs (pr_{BDM}),the standard deviation of QTL effect sizes (QTL_{SD}) the
193 recombination rate (r), and the rate of climate change (Δ). We varied each parameter
194 independently and kept the other parameters at a default value known to permit a low
195 level of introgression in preliminary tests (Table 1). Each parameter set was replicated
196 100 times. All analyses were carried out in R 3.5.1 (R Core Team 2018) and plotting was
197 done using ggplot2 (Wickham 2016).
198 Finally, while our primary goal was testing the detrimental effects of
199 hybridization, we also examined the potential *beneficial* effects of climate change
200 induced introgression, i.e. to what degree introgression facilitates adaptation. To do
201 this, we ran simulations varying the rate of climate change with (m=0.01) or without
202 (m=0) migration. At the last generation (gen=10,100), we compared the average climate
203 phenotype to the current phenotypic optimum. We defined "adaptational lag" as the
204 difference between these values divided by the rate of climate shift. This represents how
205 many generations behind the current generation that the population is adapted to. For
206 example, assume the optimum increases by 2 per generation and is currently 100, if the
207 average phenotype is 90, then the adaptational lag is 5 (e.g. (100 - 90) / 2).
208
209

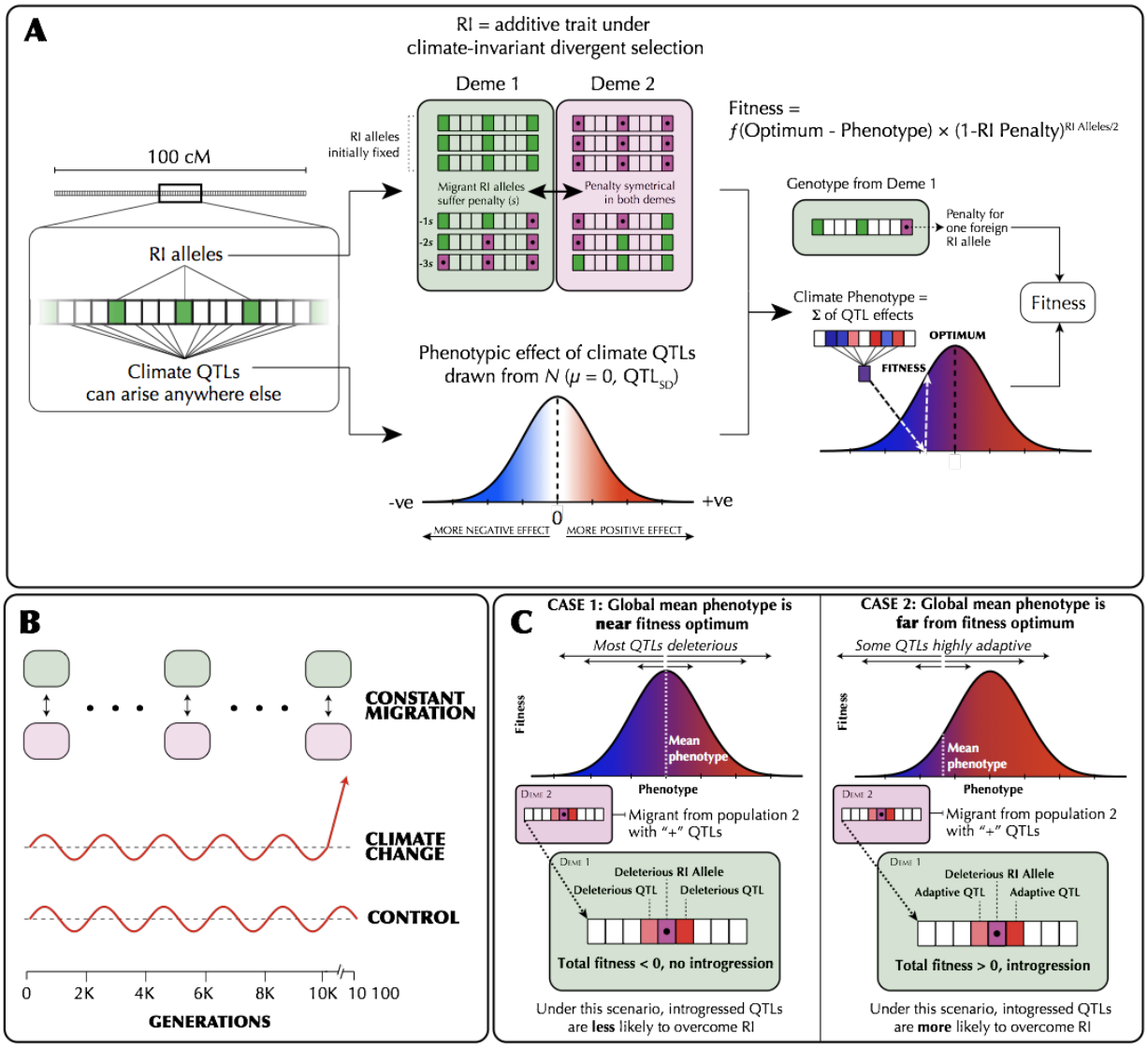

Figure 1 | (A) The genetic architecture of adaptation and speciation in the model. From left to right: Each individual has a single 100-1000 cM chromosome, over which reproductive isolation (RI) loci occur at regularly-spaced intervals. These loci are initialized with RI alleles (at 100% frequency) that confer local adaptation to one of two initial demes (depicted as green or purple/dotted alleles, corresponding to Deme 1 or Deme 2 environments). Both demes are of equal size (*Ne* = 1000). All non-RI loci (depicted as white/transparent loci, initially) have the potential to give rise to climate-adaptation alleles. The phenotypic effects of each these alleles are drawn from a normal distribution (shown as a gradient from blue to white to red). An individual's climate phenotype is the sum of the phenotypic effects of its climate QTLs (pure additivity). The fitness of each individual is a function of the number of foreign RI alleles and the phenotypic distance of that individual from the environmental optimum, with the climate fitness landscape modelled as a gaussian distribution (shown as a gradient from blue to red). (B) The course of the simulation. Migration rate and population size of the two demes is held constant. In each replicate

simulation, the fitness optimum fluctuates regularly for a 10 000-generation burn-in period. The state of the initial population is then duplicated and subjected to 100 additional generations of (1) a climate change scenario in which the climatic optimum rapidly shifts in a single direction and (2) a control scenario in which the optimum continues its fluctuation course. (C) The conditions under which adaptive introgression overwhelms RI. On the left, if the two populations are able to individually track the climatic optimum, newly-arising climate alleles are only able to exert either weakly positive or (more commonly) negative effects on fitness due to overshooting the optimum. In contrast, on the right, if the populations cannot effectively track the optimum, there is scope for climatic alleles to have large positive fitness effects. If these fitness effects are sufficiently large, these alleles can overwhelm the negative fitness effects of linked RI alleles and introgress between demes, degrading overall reproductive isolation.

Table 1 | Parameters of the adaptive introgression simulations. For each set of simulations, each parameter was set to the starting value which was varied from the minimum to maximum value by the specified increment.

Parameter	Symbol	Starting value	Range, Increment
Migration rate (proportion migrants/generation)	m	0.01	0.0-0.1, 0.001
Strength of RI	s_{RI}	0.01	0.004-0.0195, 0.0005
Number of RI loci	l	100	5-100, 5
Mutation rate (mutations/sample/locus/generation)	μ	1e-7	$1e^{-8}$-$5e^{-7}$, $1e^{-8}$
Climate QTL standard deviation	QTL_{SD}	1	0.1-5.0, 0.1
Delta	Δ	1	0.1-3, 0.1
Recombination rate	r	1e-5	$1e^{-5}$-$5e^{-5}$, $1e^{-6}$
Proportion BDM loci	BDM_{pr}	0	0-0.96, 0.04
Population size	N_e	1000	-
Environmental fitness standard deviation	$sd_{climate}$	2	-
Burn in generations	-	10000	-
Shift generations	-	100	-
Replicates	-	100	-
Loci on chromosome	-	99999	-

Burn in oscillation rate	f	1000	-
Burn in oscillation height	a	5	-

Results

Rapid climate change and adaptive introgression facilitates collapse of species boundaries

When climate change is rapid, we find that adaptive introgression of climate QTL alleles rapidly drives the homogenization of allele frequencies at linked RI loci between species. Figure 2 visualizes one example simulation where after 100 generations of climate change, RI is degraded to nearly half its original strength (Figure 2A) and introgressed climate QTL alleles are common (Figure 2B). As climate QTL alleles move between populations, RI and neutral alleles hitchhike along with them resulting in substantial genome-wide introgression (Figure 2A & 2C). In contrast, in the control scenario without climate change, RI remains intact and introgression is minimal (Figure 2 E-H).

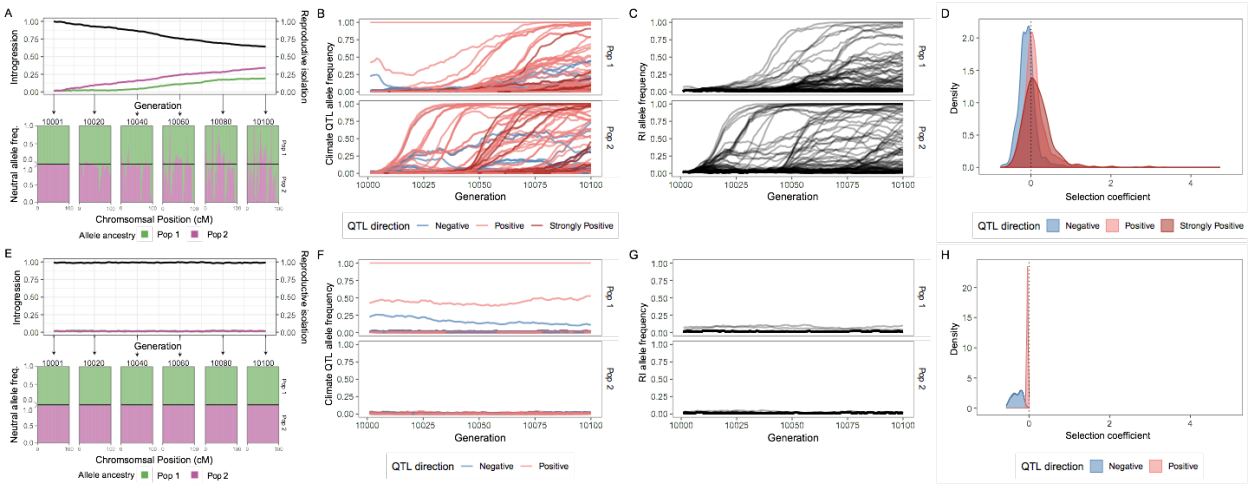

Figure 2 | A single example simulation with $\Delta = 1.5$, illustrating the climate driven adaptive introgression. Panels A-D present the test climate change scenario, while E-H are the control scenario. (A & E) The upper half is the average introgressed ancestry for each population (purple and green) and the average reproductive isolation between populations (black). The lower half is the ancestry for neutral loci during

the post-burn in period at 20 generation intervals. The top and bottom parts of this portion represent population 1 and 2 respectively. (B & F) The allele frequency trajectory for introgressed climate QTL color coded by QTL strength. Color codes QTL effect; -ve phenotypic effect (blue), +ve effects (light red) or large +ve effect (>2, dark red). (C & G) The allele frequency trajectory for introgressed RI alleles (D & H) The distribution of selection coefficients on QTL loci per population per generation. Color groups represent QTL with -ve phenotypic effect (blue), +ve effects (light red) or large +ve effect (>2, dark red). Plot is filtered to only include loci with allele frequency < 0.9 and > 0.1.

For a wide range of parameters we find decreased reproductive isolation and increased introgressed ancestry under the climate change scenario (Figures 3 and S1). This effect is enhanced by reduced levels of genetic variation; both reducing mutation rate and reducing the standard deviation of the climate QTL effect size increases the likelihood and magnitude of adaptive introgression (Figure 3A, Figure 3D). Increased migration generally causes increased RI loss, although high migration degrades RI even in the absence of climate shifts (Figure 3C). Interestingly, increasing the average fitness effect of RI loci has minimal effect on the amount of RI lost, although below a threshold, populations merge and all RI is lost during the burn in period (Figure 3G). Recombination rate has two effects; during the burn in, increased recombination allows for more RI loss, while during climate change decreased recombination leads to slightly more RI loss (Figure 3F). When varying the genetic architecture of RI, we find that fewer strong RI loci, lead to less RI loss (Figure 3H). We find that intrinsic isolation is much less effective at maintaining RI during the burn in period, consistent with previous simulations (Bank et al. 2012). Climate change increases the amount of introgression and RI loss when intrinsic isolation is present unless populations are already completely merged (Figures 3E, S1E). Lastly, increasing the rate of climate change in the test scenario increases the amount of adaptive introgression (Figure 3B).

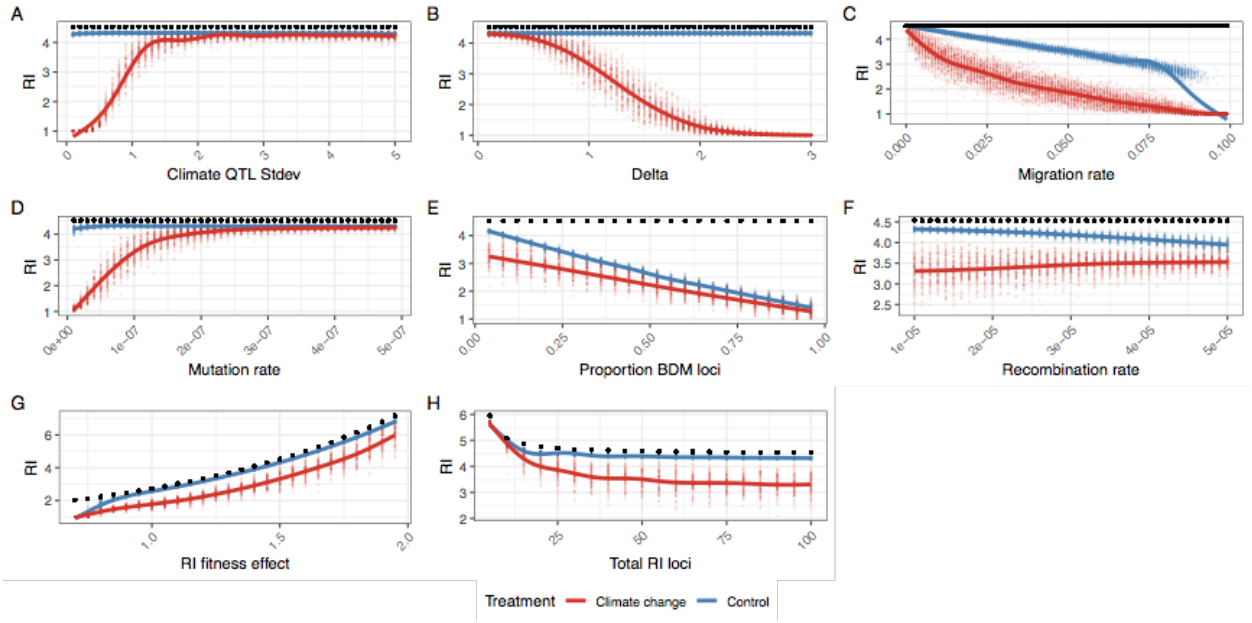

Figure 3 | The average reproductive isolation at generation 10,100 for climate change (red) and control simulations (blue), while varying individual parameters. RI is defined as the home fitness advantage which is the fold fitness advantage for the average sample in its home environment compared to the alternate environment based on divergent selection and BDM loci. A value of 1 means equal fitness in both environments and there is no RI. The black dot is the initial and maximum level of RI for each simulation. Individual parameters were varied to show the effect of (A) climate QTL effect size standard deviation, (B) optimum shift per generation (delta), (C) migration rate, (D) climate QTL mutation rate, (E) proportion of RI loci that are BDM instead of extrinsic, (F) the recombination rate, (G) the fitness effect of each RI loci and (H) the number of RI loci.

Simulation parameters fall within realistic ranges

To better connect our simulation results with observations from natural populations, we measured the rate of phenotypic evolution in the test scenario in Haldanes (standard deviations per generation). We find that most simulations had average evolutionary rates ranging from 0.01 to 0.06 Haldanes and are well within the range of empirical estimates from natural populations (Hendry et al. 2008). That said, in simulations with very high rates of climate change (Δ>2.5), we found large and erratic evolutionary rates. For many of these simulations, one or both species failed to track the

changing environment causing fitness of all individuals to fall to zero and end the simulation.

In example simulations, we found that 99.3% of the realized selection coefficients for introgressed climate QTL alleles fell below 1 (Figure 2D). QTL alleles with positive and strongly positive phenotypic effects were more likely to have positive selection coefficients, consistent with the importance of the climate optimum.

Beneficial effects of introgression

We find that migration can reduce adaptational lag when climate change is moderate or high (Figure 4). This effect is particularly strong when climate change is rapid.

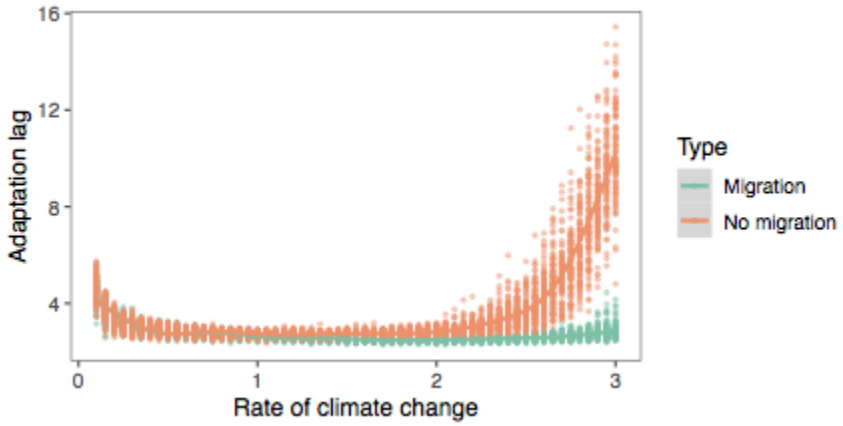

Figure 4 | The adaptational lag at the final generation for simulations with (m=0.01) and without migration (m=0). Adaptational lag is defined as the phenotypic optimum minus the phenotypic mean divided by the rate of change in optimum, and represents how many generations behind the changing optimum that the population is.

Discussion

Global climate change is expected to have wide-ranging detrimental effects on biodiversity. The movement of beneficial alleles between species, i.e. interspecific

318 adaptive introgression, is likely to increasingly relevant as the climate warms. In spite of
319 increased interest in adaptive introgression per se, we still have a poor understanding of
320 the incidental effects of adaptive introgression on the integrity of species boundaries.
321 Our simulations have shown that it is possible for adaptation to a common, changing
322 environment to cause introgression and speciation reversal. Importantly, we observed
323 this effect in scenarios where the mechanism of RI is itself completely independent of
324 the changing climate.
325
326 *Will adaptive introgression lead to speciation reversal?*
327 In our simulations, several parameters had a strong effect on the amount of
328 introgression. When adaptive variation is limited, RI is initially weak, or environmental
329 change is rapid, complete genetic homogenization is likely. In these cases, RI is
330 completely degraded and would clearly represent speciation reversal in a natural system.
331 In more moderate parts of parameter space, introgression is increased during
332 environmental change, but populations do not completely homogenize (Figure S1). In
333 these cases, RI is still eroded between populations (Figure 3). Importantly, we believe
334 our estimates of RI loss are likely somewhat conservative, because we do not include
335 any additional factors that would contribute to species collapse (e.g. cases where RI is
336 directly affected by a change in climate).
337 We found that in the absence of divergent selection intrinsic epistatic isolation
338 (BDM incompatibilities) were unable to maintain RI during the burn in period. This
339 result is consistent with previous modelling of parapatric speciation (Barton &
340 Bengtsson 1986, Bank et al. 2012, Lindtke & Buerkle 2015). Consistent with their effect

in the burn in period, during climate change, introgression and RI loss is enhanced when intrinsic RI is present. Thus, although we have focused on extrinsic RI, intrinsic RI is also susceptible to adaptive introgression.

The ultimate question of which species are in danger of reverse speciation is dependent on a multitude of interacting factors and is beyond the scope of this paper, but we can highlight several risk factors.

(1) For hybridization to be an issue, a potential hybridizing species must be at least in parapatry. Surveys have estimated the percent of species that hybridize with at least one other congener to be around 10-25%, although if climate change disrupts species ranges or premating isolation, that number may increase (Mallet 2005).

(2) The rate of environment change and the steepness of the changing fitness landscape. Species with broader climate niches will be less susceptible because they will be under weaker selection.

(3) The genetic architecture of climate adaptation in the species. Species with numerous large effect climate adaptation alleles segregating within their gene pool will be more able to adapt to the changing climate *without* introgressed alleles. Low diversity species will be more susceptible and reliant on adaptive introgression.

(4) The genetic architecture of reproductive isolation between species. Species with few large effect RI loci will be more resistant to RI decay than species with a more diffuse and polygenic RI architecture.

(5) The demographic and life history of the species. Unbalanced population sizes may result in one population harboring more adaptive alleles and lead to unbalanced introgression. Small populations will also be more susceptible to extinction due to the fitness costs of introgressed RI alleles. Features that reduce effective population size, e.g. high variance in reproductive success, are also likely to have reduced diversity of climate adapting alleles.

Implications for the fate of species in changing environments

Our simulations suggest that rapidly changing environments can cause the collapse of species barriers in the *absence* of any direct effect on the underlying strength of reproductive isolation. By design, we modelled a scenario in which the strength of RI (modelled as divergent selection) is (a) invariant throughout (i.e. not reduced by environmental change itself) and (b) totally orthogonal to the strength of climate-mediated selection (i.e. extrinsic RI alleles do not affect the climate phenotype). This is an important departure from previous work, in which the collapse of reproductive isolation or "reverse speciation" occurs because RI is itself dependent on the environment (e.g. trophic or sensory niche).

This difference has several important implications. For one, the mechanism we outline here can occur in any population where adaptive introgression is possible (i.e. RI is not absolute and the climate-mediated selective optimum is to some degree shared). This greatly expands both the number of populations that may be susceptible to introgressive collapse and the potential severity of such collapses. For example, adaptive introgression could act in concert with the collapse of climate-mediated reproductive

386 barriers, accelerating collapse. Further, while we focused on extrinsic isolation, our
387 simulations show that scenarios where reproductive barriers are independent of
388 ecological context (e.g. in the case of purely intrinsic isolation) are not immune.
389 Although we have framed our discussion in the context of climate change, our
390 results are applicable to any strong, consistent, and shared selective event. These events
391 include any environmental or ecological disturbance that alters the shared selective
392 landscape of the two populations such that both populations are sufficiently displaced
393 from their selective optima (thereby increasing the average size of selection differentials
394 between genotypes, i.e. the strength of selection). One such event that has been studied
395 in natural systems is eutrophication, which has been suggested to have caused
396 speciation reversal in European lake whitefish (Vonlanthen et al. 2012). Thus far, this
397 reversal has been attributed to changes in RI as a direct result of ecological and/or
398 behavioural changes. However, if eutrophication exerts a common selective pressure on
399 a group of parapatric species (e.g. mediated through changes in water chemistry)
400 introgression could become adaptive and contribute to the collapse of species
401 boundaries. Similarly, ocean acidification could be a strong source of shared selection
402 and may induce introgression between previously well isolated species (Pespeni et al.
403 2013).
404 In contrast to our hypothesis of introgression driving species collapse, adaptive
405 introgression of an insecticide-resistance mutation in *Anopheles* mosquitoes lead to the
406 homogenization of previously differentiated genomic region, but not genome wide
407 despeciation (Clarkson et al. 2014). In this example, selection seemingly only acts on a
408 single large effect locus, rather than the polygenic architecture of climate adaptation we

hypothesize. This limits the amount of introgression in comparison to our simulations and highlights the importance of the genetic architecture of climate adaptation.

Introgression and extinction

Here we've focused on the possibility of species collapse, but another more common predicted effect of climate change is extinction. In our model, population sizes are constant and fitness is relative, so extinction is impossible. Despite this, our results do have implications for the likelihood of extinction.

If RI alleles contribute to local adaptation (i.e. are extrinsic), then the collapse of RI must result in the spread of fitness reducing maladaptive non-local loci introgress, similar to the concept of linkage drag in plant breeding (Zamir 2001). The net effect of the introgression is positive in our climate change scenario, since the maladaptive introgressed alleles are linked to positive climate QTL alleles, but the overall fitness of the population is lower than it would be if it adapted *without* introgression. In this way, adaptive introgression makes populations better adapted to the changing climate, but less adapted to their home niche. In the real world, this may be reflected in reduced population size or growth rate and could increase the chance of extinction. This effect is dependent on the amount and type of RI loci swept to fixation by linkage with beneficial climate QTL, which in itself will depend on the speed of fixation and amount of recombination. Thus stronger selection, smaller population size or reduced recombination rate will all increase linkage drag. Note that if RI is intrinsic, this doesn't necessarily apply because intrinsic RI loci are only detrimental based on interactions with other loci and won't have any fitness penalty if all RI alleles are homogenized by introgression.

On the other hand, it is likely that the adaptive introgression of climate QTL increases the chances that a species can adapt to a changing environment instead of going extinct. Again, we can't directly address this question in our model but we do see that when all introgression is prevented adaptational lag increases (Figure 4). This is consistent with the larger total gene pool of adaptive variants available when gene flow is possible. The magnitude of this effect will depend on the amount and architecture of divergently selected loci (i.e. the potential linkage drag) as well as the diversity of climate QTL alleles in each species (i.e. the effective population size).

Linkage and the genetic architecture of climate adaptation

A key aspect of our model is that while RI loci occur at predefined intervals in the genome, climate-sensitive alleles can arise at any other locus in the genome. This allows for climate-sensitive alleles to become readily linked to RI-causing alleles and eventually introgress if the combined effect of positively selected climate alleles exceeds the deleterious effect of the linked RI allele. The incidental establishment of this linkage within the two adapting populations is a fundamental cause of later introgressive collapse. This is supported by our simulations that varied the number of RI loci and also incidentally varied the average degree of linkage between all climate-sensitive loci and all RI loci. We found that in simulations with more RI loci, and therefore a higher probability of linkage between RI and climate-sensitive loci, there was greater loss of reproductive isolation. Thus, a key question is whether such linkage could plausibly be established in a natural population.

Several lines of evidence suggest that this is likely to be true. First, the genetic architecture of adaptation to a changing climate is likely to closely resemble the

455 architecture of local adaptation in general, i.e. a large number of small effect alleles with
456 a smaller number of large effect loci (reviewed in Savolainen et al. 2013). This idea is
457 directly supported by recent work showing that climatic adaptation in conifers is
458 underlain by large number of loci scattered throughout the genome, with the majority of
459 these showing modest phenotype-environment correlations (Yeaman et al. 2016).
460 Secondly, recent analyses of large human datasets support the idea that most complex
461 traits (of any kind) are probably determined by a large number of small-effect loci found
462 nearly everywhere in genome along with a handful of "core genes" (Boyle et al. 2018).
463 Thus, given that the genetic architecture of RI is itself likely to be highly polygenic
464 (further discussed in Ravinet et al. 2017), it seems highly plausible that linkage between
465 climate-sensitive alleles and RI alleles can readily occur in natural populations.

466 *The role of recombination rate*

467 Recombination rate is thought to play a key role in mediating patterns of
468 divergence and introgression in natural populations (e.g. Samuk et al. 2017, Schumer et
469 al. 2018). Specifically, regions of high recombination are thought to be less resistant to
470 gene flow because of decreased linkage between alleles conferring RI. We see this in our
471 simulations, as simulations with higher recombination rates have greater amounts of
472 introgression in both control and climate change scenarios. Interestingly, we observe a
473 slight negative correlation between recombination rate and loss of RI under the climate
474 change scenario (Figure 3, Figure S1). This effect is a direct consequence of lower
475 recombination rates leading to increased linkage between RI alleles and globally-
476 adaptive climate alleles. This increased linkage leads in turn to larger numbers of RI
477 alleles being dragged along with globally-adaptive alleles and homogenized between

478 populations. While mutations were not particularly limiting in our simulations, adaptive
479 introgression in regions of low recombination should generally require larger effect
480 alleles than introgression in regions of high recombination, particularly at the onset of
481 climate change when selection is weaker overall.

482 *The strength of climate-mediated selection*

483 A strong shared selection pressure is ultimately the key mediator of the collapse
484 of RI we observed. Was the magnitude of simulated selection necessary to cause this
485 collapse realistic? One way to assess this is to measure the magnitude of the phenotypic
486 response to selection in our simulations and compare it to estimates from natural
487 systems. In our case, the phenotypic response to selection ranged from 0.01-0.06
488 Haldanes (standard deviations per generation). This is in line with the magnitude of
489 phenotypic response observed in both natural and anthropogenically-induced selection
490 (e.g. Hendry et al. 2008). Further, this is below the theoretical threshold of 0.1 Haldanes
491 thought to result in an unsustainable long-term response to selection (for $N_e = 500$;
492 Lynch & Lande, 1993; Bürger & Lynch, 1995).

493 Another way of assessing the realism of our scenarios is comparing the selection
494 coefficients of climate QTL in our simulations with values measured in empirical
495 studies. We measured selection coefficients in our example simulation by comparing
496 relative fitness values for samples with and without each mutation (Appendix 1), and
497 therefore are capturing not just the effect of the climate QTL mutation, but also all
498 linked loci. Only 0.7% of introgressed climate QTL loci had selection coefficients > 1,
499 within the range of empirical values, therefore adaptive introgression is occurring
500 without abnormally high selection coefficients (Kingsolver et al. 2001).

Thus, the strength of selection we modelled was not particularly extreme nor would it necessarily lead to the extinction of the modelled populations. It is also worth noting that the estimated rate of phenotypic change in wild populations due to future GCC is thought to be at least as large as the rates we described here, and are projected to likely exceed 0.1 Haldanes in many cases (Gienapp, Leimu, & Merilä, 2007; Merilä & Hoffman 2016). In sum, the global strength of phenotypic selection simulated here was not unrealistically high, and if anything represents a conservative adaptive scenario.

Conclusion

Hybridization is a double-edged sword under rapid environmental change. It can allow species access to a larger pool of adaptive alleles but linkage with RI alleles will weaken overall RI and may lead to speciation reversal. Importantly, our work highlights the dangers of hybridization for a much wider pool of species, not just those on range margins or with existing porous species boundaries. In the longer term, we predict that specific cases of speciation reversal should be linked to climate change but we also predict effects before full speciation reversal. If our model is correct, we predict that alleles conferring adaptation to present and future climate (e.g. heat or drought) will be more likely to introgress between species. Although identifying all the loci underlying climate adaptation is challenging, recent work by Exposito-Alonso et al. (2019) highlights that it can be done. Such an approach can be combined with sequencing data in related species to identify where introgression is occuring. Our results also suggest that hybrid zones should become increasingly porous as climate adaptation alleles move between species and that this effect would be stronger in regions with more dramatic

524 climate change (e.g. the arctic). This could be done by resampling previously studied
525 hybrid zones or by comparing contemporary samples to museum and herbarium
526 samples. Confirmation of these predictions would show that climate adaptation is
527 occurring through a larger multi-species gene pool and be a warning sign for the future
528 homogenization of these species.
529
530 *Acknowledgements*
531 This work was supported by an NSERC Banting Postdoctoral Fellowship to GLO and an
532 NSERC Postdoctoral Fellowship to KS. KS was further supported by postdoctoral
533 funding and good vibes from Mohamed Noor at Duke University. Matthew Osmond,
534 Kate Ostevik and Loren Rieseberg provided helpful feedback and discussions on earlier
535 versions of the manuscript. We thank Philip Messer and Ben Haller for assistance with
536 the SLiM 3.X software.
537

538 References

539
540 Abbott, R., Albach, D., Ansell, S., Arntzen, J. W., Baird, S. J., Bierne, N., ... & Butlin, R. K.
541 2013. Hybridization and speciation. Journal of evolutionary biology, 26(2), 229-
542 246.
543
544 Bank C., Bürger R. & Hermisson J. 2012. The limits to parapatric speciation:
545 Dobzhansky–Muller incompatibilities in a continent–island model. Genetics.
546 191(3):845-863.

547 Barton N. H., 1979. The dynamics of hybrid zones. Heredity. 43(3):341–359.
548

549 Barton N. H., 2013. Does hybridization influence speciation? Journal of Evolutionary
550 Biology. 26(2):267–269.
551
552 Barton, N. & Bengtsson, B.O. 1986. The barrier to genetic exchange between hybridising
553 populations. Heredity. 57(3):357-376.
554
555 Bateson W. 1909. Heredity and variation in modern lights. Darwin and Modern Science.
556 85–101
557
558 Beatty, G.E., Barker L., Chen P.P., Kelleher C.T. & Provan J. 2014. Cryptic introgression
559 into the kidney saxifrage (*Saxifraga hirsuta*) from its more abundant sympatric
560 congener *Saxifraga spathularis*, and the potential risk of genetic assimilation.
561 Annals of Botany. 115(2):179-186.
562
563 Boyle, E. A., Li, Y. I., & Pritchard, J. K. 2017. An expanded view of complex traits: from
564 polygenic to omnigenic. Cell. 169(7):1177-1186.
565
566 Bürger R. & Lynch M. 1995. Evolution and extinction in a changing environment: a
567 quantitative-genetic analysis. Evolution. 49(1):151-163.
568
569 Buerkle, C.A., Morris, R.J., Asmussen, M.A. & Rieseberg, L.H. 2000. The likelihood of
570 homoploid hybrid speciation. Heredity 84: 441–451.
571
572 Chunco AJ. 2014 Hybridization in a warmer world. Ecology and Evolution. 4(10):2019-
573 2031.
574
575 Clarkson C.S, Weetman D., Essandoh J., Yawson A.E., Maslen G., Manske M., Field
576 S.G., Webster M., Antão T., MacInnis B. & Kwiatkowski D. 2014. Adaptive
577 introgression between Anopheles sibling species eliminates a major genomic
578 island but not reproductive isolation. Nature Communications. 5:4248.
579
580 Dobzhansky T. 1934. Studies on Hybrid Sterility. I. Spermatogenesis in pure and hybrid
581 *Drosophila pseudoobscura*. Zeitschrift für Zellforschung und mikroskopische
582 Anatomie. 21:169–221
583

584 Dobzhansky, T. H. 1936. Studies on hybrid sterility. II. Localization of sterility factors in
585 Drosophila pseudoobscura hybrids. Genetics. 21(2): 113.
586
587 Exposito-Alonso M., Vasseur F., Ding W., Wang G., Burbano H.A., & Weigel, D. 2018.
588 Genomic basis and evolutionary potential for extreme drought adaptation in
589 *Arabidopsis thaliana*. Nature ecology & evolution. 2(2):352.
590
591 Garroway C.J., Bowman J., Cascaden T.J., Holloway G.L., Mahan C.G., Malcolm J.R.,
592 Steele M.A., Turner G. & Wilson P.J. 2010. Climate change induced hybridization
593 in flying squirrels. Global Change Biology. 16(1):113-121.
594
595 Gerard P.R., Fernandez-Manjarres J.F., & Frascaria-Lacoste N.A. 2006. Temporal cline
596 in a hybrid zone population between *Fraxinus excelsior* L. and *Fraxinus angustifolia*
597 Vahl. Molecular Ecology. 15(12):3655-3667.
598
599 Gienapp P., Leimu R. & Merilä J. 2007. Responses to climate change in avian migration
600 time—microevolution versus phenotypic plasticity. Climate Research. 35(1-2):25-
601 35.
602
603 Gingerich P.D. 1993. Quantification and comparison of evolutionary rates. American
604 Journal of Science, 293(A):453-478
605
606 Gómez J.M., González-Megías A., Lorite J., Abdelaziz M. & Perfectti F. 2015. The silent
607 extinction: climate change and the potential hybridization-mediated extinction
608 of endemic high-mountain plants. Biodiversity and Conservation. 24(8):1843-
609 1857.
610
611 Gompert, Z., Parchman, T. L., & Buerkle, C. A. 2012. Genomics of isolation in hybrids.
612 Philosophical Transactions of the Royal Society of London B: Biological Sciences.
613 367(1587):439-450.
614
615 Haller B.C. & Messer P.W. 2018. SLiM 3: Forward genetic simulations beyond the
616 Wright–Fisher model, Molecular Biology and Evolution. msy228
617

618 Hendry A.P., Farrugia T.J. & Kinnison M.T. 2008. Human influences on rates of
619 phenotypic change in wild animal populations. Molecular Ecology. 17(1):20-29.
620
621 Hoffmann A.A. & Sgrò C.M. 2011 Climate change and evolutionary adaptation. Nature.
622 470(7335):479.
623
624 Jump A.S. & Penuelas J. 2005. Running to stand still: adaptation and the response of
625 plants to rapid climate change. Ecology Letters. 8(9):1010-1020.
626
627 Kingsolver, J.G., Hoekstra H.E., Hoekstra J.M, Berrigan D., Vignieri S.N., Hill C.E.,
628 Hoang A., Gibert P., & Beerli P. 2001. The strength of phenotypic selection in
629 natural populations. The American Naturalist. 3(157):245-261.
630
631 Lindtke, D. & Buerkle, C.A. 2015. The genetic architecture of hybrid incompatibilities
632 and their effect on barriers to introgression in secondary contact. Evolution.
633 69(8):1987-2004.
634
635 Lynch, M., & R. Lande. 1993. Evolution and extinction in re-sponse to environmental
636 change. Pp. 234-250 in P. M. Kareiva, J. G. Kingsolver, and R. B. Huey, eds. Biotic
637 interactions and global change. Sinauer, Sunderland, Mass.
638
639 Mallet J. 2005. Hybridization as an invasion of the genome. Trends in Ecology &
640 Evolution. 20(5):229-237.
641
642 Merilä, J., & Hoffmann, A.A. 2016. Evolutionary Impacts of Climate Change. In *Oxford*
643 *Research Encyclopedia of Environmental Science*. Oxford University Press.
644
645 Muller, H.J. 1942. Isolating mechanisms, evolution, and temperature. Biol. Symp. 6:71–
646 125.
647
648 Oliveira R., Godinho R., Randi E. & Alves P.C. 2008. Hybridization versus conservation:
649 are domestic cats threatening the genetic integrity of wildcats (*Felis silvestris*
650 *silvestris*) in Iberian Peninsula?. Philosophical Transactions of the Royal Society
651 of London B: Biological Sciences. 363(1505):2953-2961.
652

Pespeni M.H., Sanford E., Gaylord B., Hill T.M., Hosfelt J.D., Jaris H.K., LaVigne M., Lenz E.A., Russell A.D., Young M.K. & Palumbi S.R. 2013. Evolutionary change during experimental ocean acidification. Proceedings of the National Academy of Sciences. 110(17):6937-6942.

Pfennig KS. 2007. Facultative mate choice drives adaptive hybridization. Science. 318(5852):965-967.

R Core Team (2018). R: A language and environment for statistical computing. R Foundation for Statistical Computing, Vienna, Austria. URL https://www.R-project.org/.

Ravinet M., Faria R., Butlin R.K., Galindo J., Bierne N., Rafajlović M., Noor M.A.F., Mehlig B & Westram, A. M. 2017. Interpreting the genomic landscape of speciation: a road map for finding barriers to gene flow. Journal of Evolutionary Biology. 30(8):1450-1477.

Rhymer J.M. & Simberloff D. 1996. Extinction by hybridization and introgression. Annual Review of Ecology and Systematics. 27(1):83-109.

Samuk K., Owens G.L., Delmore K.E., Miller S.E., Rennison D.J. & Schluter D. 2017. Gene flow and selection interact to promote adaptive divergence in regions of low recombination. Molecular Ecology. 26(17):4378-4390.

Savolainen O., Lascoux M., & Merilä J. 2013. Ecological genomics of local adaptation. Nature Reviews Genetics. 14(11):807.

Seehausen, O. 2013. Conditions when hybridization might predispose populations for adaptive radiation. Journal of Evolutionary Biology, 26(2), 279-281.

Schumer M., Xu C., Powell D.L., Durvasula A., Skov L., Holland C., Blazier J.C., Sankararaman S., Andolfatto P., Rosenthal G.G. & Przeworski, M. 2018. Natural selection interacts with recombination to shape the evolution of hybrid genomes. Science. 360(6389):656-660.

688 Taylor E.B., Boughman J.W., Groenenboom M., Sniatynski M., Schluter D. & Gow J.L.
689 2006. Speciation in reverse: morphological and genetic evidence of the collapse of
690 a three-spined stickleback (*Gasterosteus aculeatus*) species pair. Molecular
691 Ecology.15(2):343-355.
692
693 Thomas C.D., Cameron A., Green R.E., Bakkenes M., Beaumont L.J., Collingham Y.C.,
694 Erasmus B.F., De Siqueira M.F., Grainger A., Hannah L. & Hughes L. 2004.
695 Extinction risk from climate change. Nature. 427(6970):145.
696
697 Todesco M., Pascual M.A., Owens G.L., Ostevik K.L., Moyers B.T., Hübner S., Heredia
698 S.M., Hahn M.A., Caseys C., Bock D.G., Rieseberg L.H. 2016. Hybridization and
699 extinction. Evolutionary Applications. 9(7):892-908.
700
701 Vallender R., Robertson R.J., Friesen V.L. & Lovette I.J. 2007. Complex hybridization
702 dynamics between golden-winged and blue-winged warblers (*Vermivora*
703 *chrysoptera* and *Vermivora pinus*) revealed by AFLP, microsatellite, intron and
704 mtDNA markers. Molecular Ecology. 16(10):2017-2029.
705
706 Vonlanthen P., Bittner D., Hudson A.G., Young K.A., Müller R., Lundsgaard-Hansen B.,
707 Roy D., Di Piazza S., Largiadèr C.R. & Seehausen O. 2012. Eutrophication causes
708 speciation reversal in whitefish adaptive radiations. Nature. 482(7385):357.
709
710 Walther G.R., Post E., Convey P., Menzel A., Parmesan C., Beebee T.J., Fromentin J.M.,
711 Hoegh-Guldberg O. & Bairlein F. 2002 Ecological responses to recent climate
712 change. Nature. 416(6879):389.
713
714 Wickham H. 2016. ggplot2: elegant graphics for data analysis. Springer.
715
716 Yeaman S., Hodgins K.A., Lotterhos K.E., Suren H., Nadeau S., Degner J.C., Nurkowski
717 K.A., Smets P., Wang T., Gray L.K., Liepe K.J., Hamann A., Holliday J.A.,
718 Whitlock M.C., Rieseberg L.H. & Liepe K.J. 2016. Convergent local adaptation to
719 climate in distantly related conifers. Science. 353(6306):1431-1433.
720
721 Zamir D. 2001. Improving plant breeding with exotic genetic libraries. Nature reviews
722 genetics. 2(12):983–989.

723

724 Zimova M., Mills L.S. & Nowak J.J. 2016. High fitness costs of climate change-induced
725 camouflage mismatch. Ecology Letters. 19(3):299-307.

Supplemental Figures

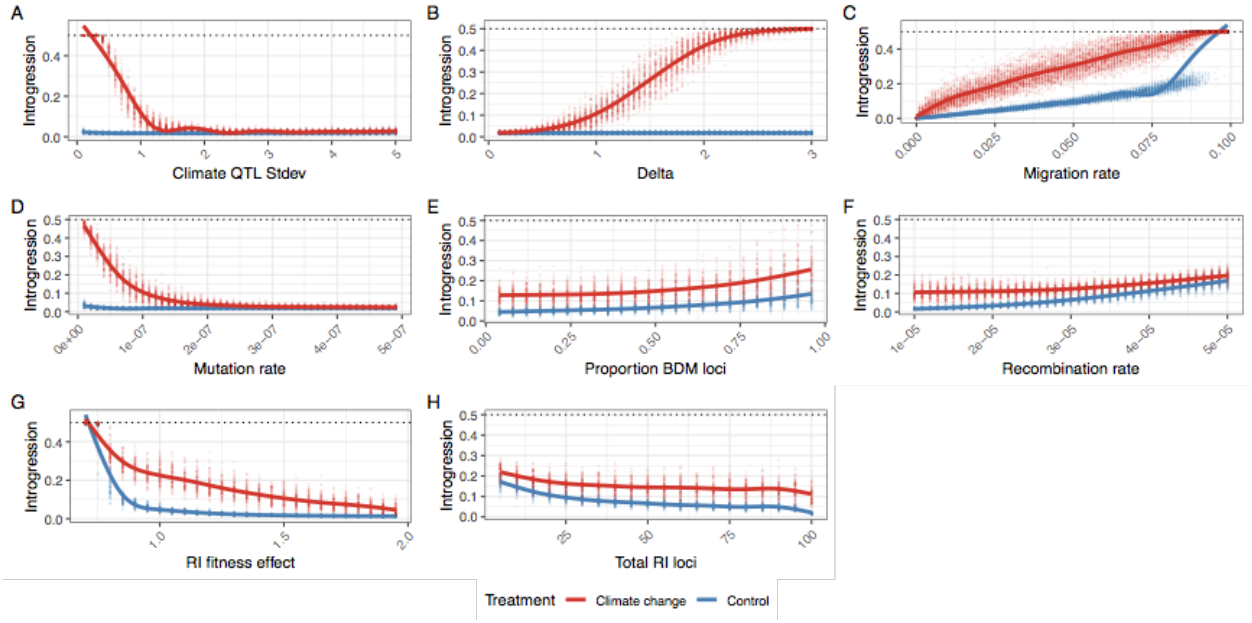

Figure S1 | The average amount of introgression at generation 10,100 for climate change (red) and control simulations (blue), while varying individual parameters. Complete homogenization of both populations occurs when average introgression = 0.5. Individual parameters were varied to show the effect of (A) climate QTL effect size standard deviation, (B) optimum shift per generation (delta), (C) migration rate, (D) climate QTL mutation rate, (E) proportion of RI loci that are BDM instead of extrinsic, (F) the recombination rate, (G) the fitness effect of each RI loci and (H) the number of RI loci.

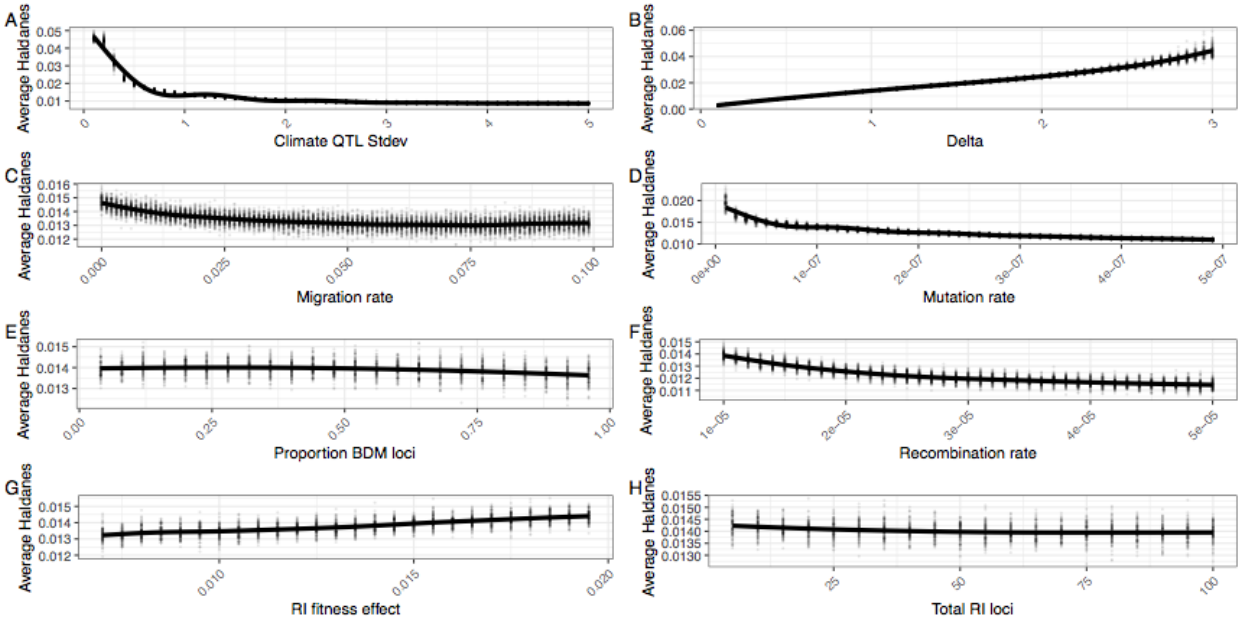

Figure S2 | The average Haldanes for the post-burn in period with climate change. Individual parameters were varied to show the effect of A) climate QTL effect size standard deviation, (B) optimum shift per generation (delta), (C) migration rate, (D) climate QTL mutation rate, (E) proportion of RI loci that are BDM instead of extrinsic, (F) the recombination rate, (G) the fitness effect of each RI loci and (H) the number of RI loci. Note that Haldanes are scaled by trait variation, so the same rate of absolute phenotypic change (i.e. Darwins) can have multiple different Haldanes if the phenotypic variability changes. In all panels except B, the rate of phenotypic change roughly matches the rate of environmental change, so the differences in Haldanes reflects differences in trait variance. Lower trait variance (e.g. through reduced mutation rate or lower QTL standard deviation) produces higher haldanes for the same absolute rate of phenotypic change.

Figure & Table Captions

Figure 1

(A) The genetic architecture of adaptation and speciation in the model. From left to right: Each individual has a single 100-1000 cM chromosome, over which reproductive isolation (RI) loci occur at regularly-spaced intervals. These loci are initialized with RI alleles (at 100% frequency) that confer local adaptation to one of two initial demes (depicted as green or purple/dotted alleles, corresponding to Deme 1 or Deme 2 environments). Both demes are of equal size (Ne = 1000). All non-RI loci (depicted as white/transparent loci, initially) have the potential to give rise to climate-adaptation alleles. The phenotypic effects of each these alleles are drawn from a normal distribution (shown as a gradient from blue to white to red). An individual's climate phenotype is the sum of the phenotypic effects of its climate QTLs (pure additivity). The fitness of each individual is a function of the number of foreign RI alleles and the phenotypic distance of that individual from the environmental optimum, with the climate fitness landscape modelled as a gaussian distribution (shown as a gradient from blue to red). (B) The course of the simulation. Migration rate and population size of the two demes is held constant. In each replicate simulation, the fitness optimum fluctuates regularly for a 10 000-generation burn-in period. The state of the initial population is then duplicated and subjected to 100 additional generations of (1) a climate change scenario in which the climatic optimum rapidly shifts in a single direction and (2) a control scenario in which the optimum continues its fluctuation course. (C) The conditions under which adaptive introgression overwhelms RI. On the left, if the two populations are able to individually track the climatic optimum, newly-arising climate alleles are only able to exert either weakly positive or (more commonly) negative effects on fitness due to overshooting the optimum. In contrast, on the right, if the populations cannot effectively track the optimum, there is scope for climatic alleles to have large positive fitness effects. If these fitness effects are sufficiently large, these alleles can overwhelm the negative fitness effects of linked RI alleles and introgress between demes, degrading overall reproductive isolation.

Figure 2

A single example simulation with Δ = 1.5, illustrating the climate driven adaptive introgression. Panels A-D present the test climate change scenario, while E-H are the control scenario. (A & E) The upper half is the average introgressed ancestry for each population (purple and green) and the average reproductive isolation between populations (black). The lower half is the ancestry for neutral loci during the post-burn in period at 20 generation intervals. The top and bottom parts of this portion represent population 1 and 2 respectively. (B & F) The allele frequency trajectory for introgressed climate QTL color coded by QTL strength. Color codes QTL effect; -ve phenotypic effect (blue), +ve effects (light red) or large +ve effect (>2, dark red). (C & G) The allele frequency trajectory for introgressed RI alleles (D & H) The distribution of selection coefficients on QTL loci per population per generation. Color groups represent QTL with -ve

phenotypic effect (blue), +ve effects (light red) or large +ve effect (>2, dark red). Plot is filtered to only include loci with allele frequency < 0.9 and > 0.1.

Figure 3

The average reproductive isolation at generation 10,100 for climate change (red) and control simulations (blue), while varying individual parameters. RI is defined as the home fitness advantage which is the fold fitness advantage for the average sample in its home environment compared to the alternate environment based on divergent selection and BDM loci. A value of 1 means equal fitness in both environments and there is no RI. The black dot is the initial and maximum level of RI for each simulation. Individual parameters were varied to show the effect of (A) climate QTL effect size standard deviation, (B) optimum shift per generation (delta), (C) migration rate, (D) climate QTL mutation rate, (E) proportion of RI loci that are BDM instead of extrinsic, (F) the recombination rate, (G) the fitness effect of each RI loci and (H) the number of RI loci.

Figure S1

The average amount of introgression at generation 10,100 for climate change (red) and control simulations (blue), while varying individual parameters. Complete homogenization of both populations occurs when average introgression = 0.5. Individual parameters were varied to show the effect of (A) climate QTL effect size standard deviation, (B) optimum shift per generation (delta), (C) migration rate, (D) climate QTL mutation rate, (E) proportion of RI loci that are BDM instead of extrinsic, (F) the recombination rate, (G) the fitness effect of each RI loci and (H) the number of RI loci.

Figure S2

The average Haldanes for the post-burn in period with climate change. Individual parameters were varied to show the effect of A) climate QTL effect size standard deviation, (B) optimum shift per generation (delta), (C) migration rate, (D) climate QTL mutation rate, (E) proportion of RI loci that are BDM instead of extrinsic, (F) the recombination rate, (G) the fitness effect of each RI loci and (H) the number of RI loci. Note that Haldanes are scaled by trait variation, so the same rate of absolute phenotypic change (i.e. Darwins) can have multiple different Haldanes if the phenotypic variability changes. In all panels except B, the rate of phenotypic change roughly matches the rate of environmental change, so the differences in Haldanes reflects differences in trait variance. Lower trait variance (e.g. through reduced mutation rate or lower QTL standard deviation) produces higher haldanes for the same absolute rate of phenotypic change.

Table 1

Parameters of the adaptive introgression simulations. For each set of simulations, each parameter was set to the starting value which was varied from the minimum to maximum value by the specified increment.